Front. Energy 2017, 11(1): 52–59
DOI 10.1007/s11708-016-0429-3

RESEARCH ARTICLE

Yanlin CHEN, Sihua ZHONG, Miao TAN, Wenzhong SHEN

SiO_2 passivation layer grown by liquid phase deposition for silicon solar cell application

Abstract Surface passivation is one of the primary requirements for high efficient silicon solar cells. Though the current existed passivation techniques are effective, expensive equipments are required. In this paper, a comprehensive understanding of the SiO_2 passivation layer grown by liquid phase deposition (LPD) was presented, which was cost-effective and very simple. It was found that the post-annealing process could significantly enhance the passivation effect of the LPD SiO_2 film. Besides, it was revealed that both chemical passivation and field-effect passivation mechanisms played important roles in outstanding passivation effect of the LPD SiO_2 film through analyzing the minority carrier lifetime and the surface recombination velocity of n-type and p-type silicon wafers. Although the deposition parameters had little influence on the passivation effect, they affected the deposition rate. Therefore, appropriate deposition parameters should be carefully chosen based on the compromise of the deposition rate and fabrication cost. By utilizing the LPD SiO_2 film as surface passivation layer, a 19.5%-efficient silicon solar cell on a large-scale wafer (156 mm × 156 mm) was fabricated.

Keywords Si solar cell, passivation, SiO_2, liquid phase deposition, carrier lifetime

Received July 8, 2016; accepted September 5, 2016

Yanlin CHEN, Sihua ZHONG (✉), Miao TAN
Institute of Solar Energy, and Key Laboratory of Artificial Structures and Quantum Control (Ministry of Education), Department of Physics and Astronomy, Shanghai Jiao Tong University, Shanghai 200240, China
E-mail: zhongsh@sjtu.edu.cn

Wenzhong SHEN (✉)
Institute of Solar Energy, and Key Laboratory of Artificial Structures and Quantum Control (Ministry of Education), Department of Physics and Astronomy, Shanghai Jiao Tong University, Shanghai 200240; Collaborative Innovation Center of Advanced Microstructures, Nanjing 210093, China
E-mail: wzshen@sjtu.edu.cn

1 Introduction

It is well known that surface passivation plays a key role in high-efficiency silicon solar cells. SiO_2 film is proved to be one of the most effective dielectric passivation layers and thus gains lots of concerns in photovoltaic industry [1,2]. In general, the SiO_2 passivation layer is thermally grown in a tube furnace or deposited by vacuum-based systems such as the expanding thermal plasma technique [3,4]. Although the SiO_2 film deposited by these approaches can effectively passivate the silicon surface, especially after annealing in forming gas [3,4], none of these methods is ideal for low-cost manufacturing. Considering the cost-effectiveness, attempts are made to find another approach to produce the high-quality SiO_2 film with low cost. Fortunately, the liquid phase deposition (LPD) for growing SiO_2 film may provide a good solution with many advantages such as low cost, simple equipment, high deposition rate and low processing temperature.

The mechanism of the LPD was originally proposed by Nagayama et al. [5]. In briefly, the deposition processing of SiO_2 is based on the hydrolysis reaction of silica-supersaturated hydrofluosilicic acid written as

$$\Delta H + H_2SiF_6 + 2H_2O \leftrightarrow 6HF + SiO_2 \downarrow \qquad (1)$$

where ΔH means that the positive reaction is an endothermal reaction. When the reactants (hydrofluosilicic acid and water) are excessive, the equilibrium reaction will shift from left to right, resulting in the precipitation of SiO_2. In recent years, there are lots of reports on LPD SiO_2 film [6–14]. Most of the reports focus on investigating the effect of growth conditions involving the growth temperature, the solution concentration and the growth time on the characters of the LPD SiO_2 film. Up to the present, the LPD SiO_2 film is mainly applied to microelectronics as dielectric insulating layer [10–12] but is rarely applied to solar cells as a passivation layer. Yuan et al. [13] have first tried to apply LPD SiO_2 film to silicon solar cells as the passivation layer and fabricated a 16.4%-efficient black

silicon solar cell, presenting the promising application of LPD SiO_2 film in silicon solar cells. He et al. [14] have also applied LPD SiO_2 passivation layer to multicrystalline silicon solar cells, but the passivation effect and the resulted conversion efficiency (5.61%) are not satisfying. Therefore, it is of significant importance to comprehensively understand the LPD SiO_2 passivation layer and propose the approach to realize outstanding passivation effect.

In this paper, the influence of the deposition conditions together with post-annealing treatment on the properties and passivation effect of the LPD SiO_2 film was systematically investigated. It was found that an annealing temperature higher than 700°C was required to obtain a high-quality passivation effect of the LPD SiO_2 film. Moreover, the film had an excellent passivation effect on both p-type and n-type silicon wafers but a better passivation effect on n-type, suggesting the simultaneous presence of chemical passivation and field-effect passivation. Though the deposition conditions did not have much influence on the passivation effect of the LPD SiO_2 film, they affected the deposition rate. A medium concentration of H_2SiF_6 (1.5 M) and a medium temperature (50°C) were suggested to be the optimal deposition conditions based on the tradeoff of material cost, thermal cost and deposition rate. This optimized LPD SiO_2 film was successfully applied to silicon solar cells as the front surface passivation layer, achieving a convention efficiency of 19.5% on a large scale (156 mm × 156 mm).

2 Experimental details

2.1 Deposition of SiO_2 film

The whole deposition system mainly consists of a Teflon beaker containing a silica-supersaturated hydrofluosilicic acid (H_2SiF_6) solution, a holder for holding silicon wafers and a magnetic stirring apparatus (90-18, Shanghai Sile Instrument Co., Ltd.). The solution temperature was controlled by using the water bath method. To prepare the silica-supersaturated H_2SiF_6 solution, silicic acid powders (99.9%, Sigma-Aldrich) were added to a raw H_2SiF_6 solution (33.5%–35%, Sigma-Aldrich) and stirred at 400 r/min for 20 min at room temperature to obtain the silica-saturated H_2SiF_6 solution. The concentration of H_2SiF_6 in the silica-saturated solution was 3.09 M. Then, an appropriate amount of deionized (DI) water was added to the silica-saturated H_2SiF_6 solution to form the silica-supersaturated solution which was directly used for the SiO_2 deposition. The concentration of H_2SiF_6 in the supersaturated solution was controlled by the amount of the DI water added. The substrates utilized for SiO_2 deposition were Czochralski (Cz) silicon with a resistivity of 1–3 Ω·cm for p-type and 3–4 Ω·cm for n-type and a thickness of 200 μm. Before depositing SiO_2 film, the substrates were pretreated by being dipped into diluted HF solution and diluted HCl solution to remove the natural silicon dioxide and metallic ions, and then immersed into DI water to gain OH-terminated surface, which substantially facilitated the growth of the SiO_2 film [6]. After these pretreatments, the silicon wafers were immersed in the supersaturated solution with the controlled concentration of H_2SiF_6 and temperature to deposit SiO_2 films.

2.2 Fabrication of silicon solar cells

For the fabrication of silicon solar cells, the crystalline silicon was Cz p-type with a resistivity of 1–3 Ω·cm, a thickness of 200 μm and an area of about 238.95 cm^2 (quasi-square: 156 mm × 156 mm). After surface texturization and p-doping steps, the phosphorosilicate glass (formed in the doping process) on the rear side was removed in the HF solution first. Then, the silicon wafers were immersed in tetramethylammonium hydroxide solution to produce polished rear surface. Next, the phosphorosilicate glass on the front side was removed and the SiO_2 films were deposited on both sides of the wafers by the LPD. The wafers were annealed in a muffle furnace at the annealing temperature of 800°C for 5 min to obtain a high-quality passivation effect and subsequently the SiO_2 film on the back side was removed by using the HF. After that, SiN_x coatings were deposited on the SiO_2 films as the antireflection layers by plasma enhanced chemical vapor deposition. Finally, the electrodes were fabricated on both the front and back sides by screen printing technique and co-fired in firing furnace.

2.3 Characterizations

The effective minority carrier lifetime (τ) of the Si wafers symmetrically passivated by the LPD SiO_2 film was measured by using the Semilab WT-1200A lifetime tester, which directly reflected the passivation quality. The thermolyne muffle furnace was used to study the impact of post-annealing on the surface passivation effect of the LPD SiO_2 films. The surface morphologies of the LPD SiO_2 films on different substrates were observed by using the scanning electron microscope (SEM). The element compositions and chemical configuration of the LPD SiO_2 films were characterized by using the X-ray photoelectron spectroscopy (XPS), and using monochromatic Al K_α radiation as the X-ray source. The infrared absorption spectra were measured by using the Fourier transform infrared (FTIR) spectrometer in the range of 350 to 8000 cm^{-1}. The refractive index and thickness of the LPD SiO_2 films were determined by using the spectroscopic ellipsometry. The current (I)–voltage (V) tester was used to measure the electrical performances (I–V and power (P)–V curves) of the LPD SiO_2 passivated solar cell under AM1.5 spectrum at the temperature of 25°C.

3 Results and discussion

3.1 Quality of LPD SiO_2

SiO_2 films were successfully fabricated by the LPD under different growth conditions. For the morphological observation and the identification of the chemical composition, the films grown at 50°C for two hours with 1.0 M H_2SiF_6 without loss of generality were chosen. Figures 1 (a) and (b) respectively show the top-view and cross-sectional SEM image of the LPD SiO_2 film deposited on the polished silicon substrate, both demonstrating that the SiO_2 film is uniformly and compactly deposited on the silicon surface. The LPD SiO_2 film was also grown on the pyramid structure textured silicon surface which was the real circumstance for commercial silicon solar cells, shown in Fig. 1(c) and (d). The SiO_2 film was conformally deposited on the whole silicon pyramid textures in spite of the size of the pyramid, which was the primary requirement for effective surface passivation. To confirm the element composition and chemical configuration of the film, the samples above were characterized by using the XPS and FTIR spectrometer. Figure 1(e) depicts the XPS full-scan spectrum of the as-prepared LPD SiO_2 film. The peak values of elementary binding energy in the spectrum are all modified by standard C 1 s peak located at 284.6 eV.

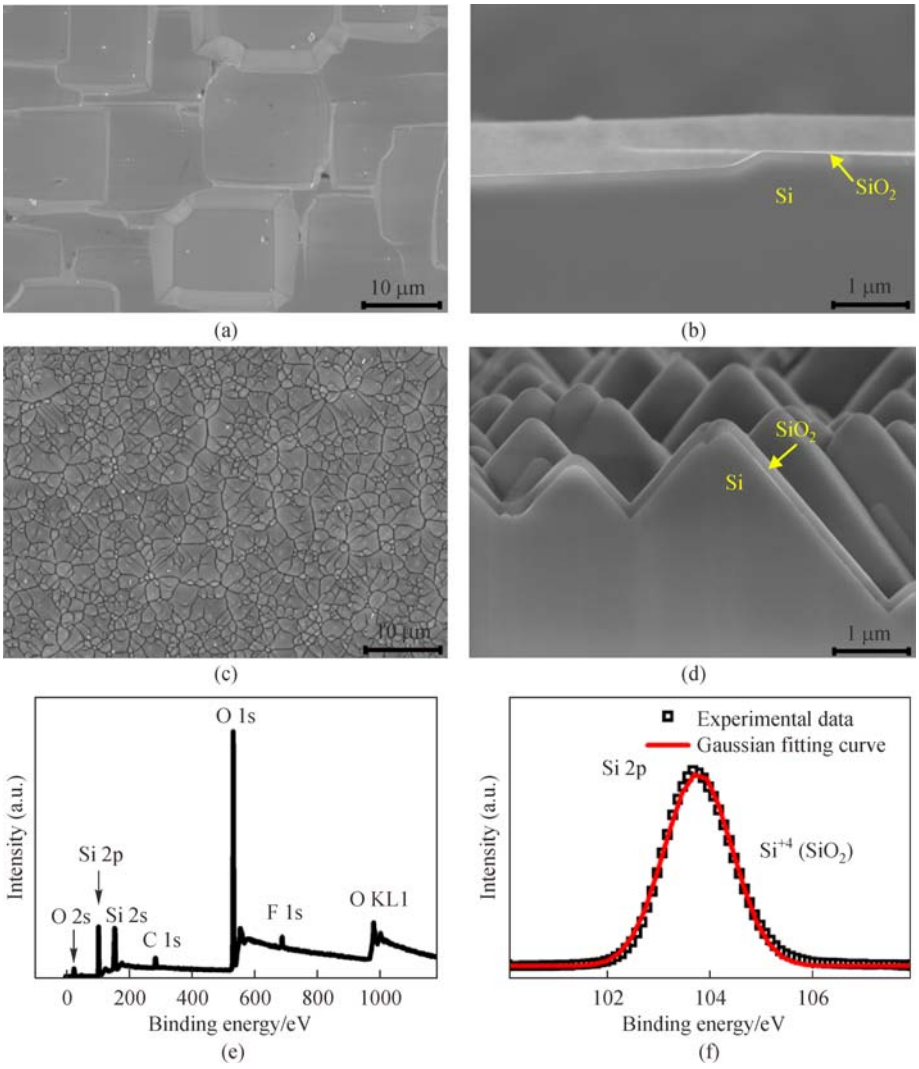

Fig. 1 Quality of LPD SiO_2 film

(a) Top-view of the LPD SiO_2 film grown on the polished silicon substrate; (b) cross-sectional SEM images of the LPD SiO_2 film grown on the polished silicon substrate; (c) top-view of LPD SiO_2 film grown on the pyramid structure textured silicon substrate; (d) cross-sectional SEM images of LPD SiO_2 film grown on the pyramid structure textured silicon substrate; (e) XPS full-scan spectrum of the as-deposited LPD SiO_2 film; (f) XPS Si 2p spectrum of the as-deposited LPD SiO_2 film (The black open squares represent the experimental data and the red solid curve is the Gaussian fitting curve based on the raw data.)

The peaks of 25.3 eV, 103.68 eV, 153.96 eV, 284.6 eV, 532.98 eV, 688.98 eV and 979.5 eV are respectively corresponding to O 2s, Si 2p, Si 2s, C 1s, O 1s, F 1s and O KL1 [15–17]. The carbon detected by XPS may have been induced by the external circumstance (e.g., engine oil of XPS instrument and atmosphere). The fluoride (F) comes from the H_2SiF_6 reactant, which exists in the form of Si-F bond in the film as displayed in Fig. 2(a). Other impurities are below the detection limit. Figure 1(f) shows the XPS fine-scan spectrum for Si 2p. The XPS experimental data shows a symmetric peak, which fits well with a single Gaussian peak located at 103.77 eV, revealing the chemical state of the LPD SiO_2 is silicon dioxide without any suboxide [18].

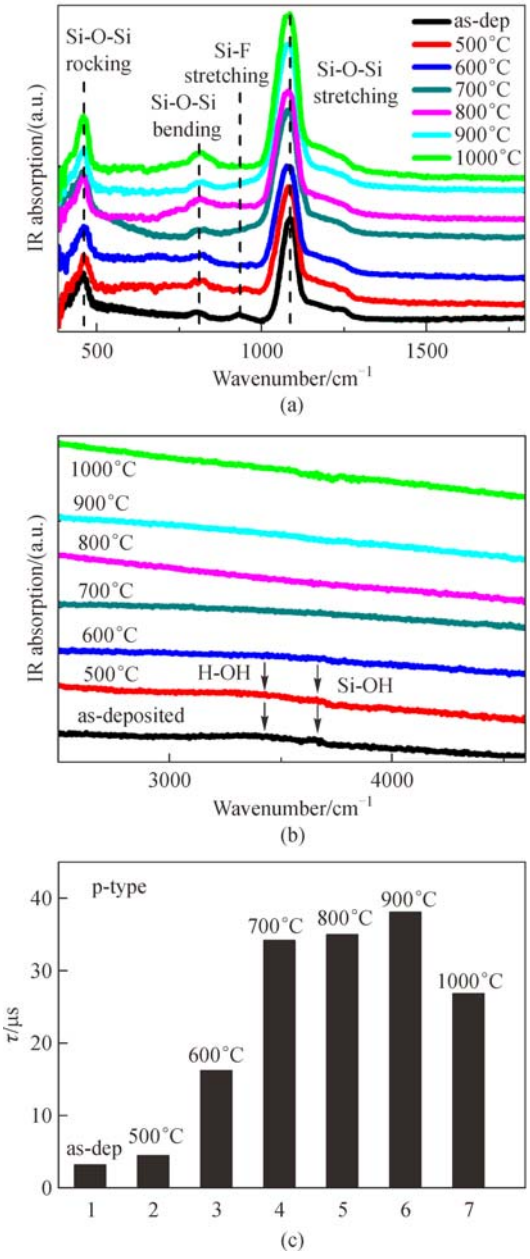

Fig. 2 Influence of annealing temperature on chemical bonds and passivation effect of LPD SiO_2 film
(a) FTIR spectra of the as-prepared LPD SiO_2 film and the LPD SiO_2 film annealed at different temperatures in the small wavenumber region; (b) FTIR spectra of the as-prepared LPD SiO_2 film and the LPD SiO_2 film annealed at different temperatures in the large wavenumber region; (c) histogram of τ of the as-deposited and post-annealed samples (as-dep represents as-deposited)

Figure 2((a) and (b)) further displays the FTIR absorption spectra of the as-prepared LPD SiO_2 film (black curves). The characteristic peaks at 457 cm^{-1}, 800 cm^{-1} and 1085 cm^{-1} are corresponding to the Si-O-Si rocking vibration mode, the Si-O-Si bending vibration mode, and the Si-O-Si stretching vibration mode, respectively [10,11,19]. The absorption peak at 931 cm^{-1} may be attributed to the Si-F stretching vibration mode [10,11]. Additionally, as exhibited in Fig. 2(b), the infrared absorption signal in the range of 3000 cm^{-1} to 4000 cm^{-1} is related to the OH-group vibration [10,19]. In detail, the weak peak at 3670 cm^{-1} corresponds to the Si-OH stretching vibration mode while the absorption band at 3400 cm^{-1} is attributed to the H-OH stretching vibration. No other prominent vibration modes are found in the spectrum from 350 cm^{-1} to 8000 cm^{-1}, well according with the result of XPS in Fig. 1.

3.2 Influence of annealing process

To study the effect of the post-annealing on the properties of the LPD SiO_2 films, the samples, which are the double-sided polished p-type Si wafers with the LPD SiO_2 films on both sides, were subjected to anneal at different temperatures in atmosphere for 5 min by muffle furnace. The annealed samples were also characterized by FTIR spectrometer, as shown in Fig. 2(a) and (b). Obviously, the signals of the Si-F, Si-OH and H-OH stretching vibration modes almost disappear after annealing at the temperatures higher than 700°C, contrasting to the gradually increased intensity of the Si-O-Si stretching vibration mode with the annealing temperature. The reason for this is that at a rather high annealing temperature, the Si-F bond and Si-OH bond break and transform to the Si-O-Si bond and HF, and the latter escapes away from the LPD SiO_2 films by evaporation. As a result, the element composition of the post-annealed LPD SiO_2 film is highly pure. In addition, compared with the spectrum of the as-deposited sample, the peak of the Si-O-Si stretching vibration mode slightly shifts to the lower wave number (red shift) after annealing. It is known that the Si-O-Si stretching vibration mode is closely related to the composition or the density of the SiO_2 film [20]. Therefore, it can be inferred that the increased density of the post-annealed SiO_2 film (which is verified by the increased refractive index, as shown in Fig. 3 and Fig. 4) should be responsible for the red shift of the Si-O-Si stretching vibration frequency in the study.

The passivation effect of the LPD SiO_2 films before and

after annealing was characterized by lifetime tester, as presented in Fig. 2(c). The τ of the as-deposited sample is only 3.18 μs, similar to that of a naked Si wafer (1.7 μs), indicating the rather poor surface passivation effect of the as-deposited SiO_2 film. However, the surface passivation ability of the LPD SiO_2 film can be effectively improved by the annealing process. The τ of the post-annealed samples gradually increases with the annealing temperature from 500°C to 700°C and then keeps a value of around 35 μs at the annealing temperature of 700°C to 900°C. This improved τ may be attributed to the reconstruction of the Si/SiO_2 interface which makes the dangling bonds on Si wafer surface effectively passivated. However, the passivation effect of the SiO_2 film begins to decrease at a higher annealing temperature of 1000°C. To better understand the function of post-annealing, the silicon wafers were also passivated by other wet oxidation methods (H_2O_2 oxidation and HNO_3 oxidation) and made to go through the same annealing process (800°C, 5 min). However, the τs are only 19 μs and 8 μs for HNO_3 oxidized wafer and H_2O_2 oxidized wafers, respectively. These contrast experiments explicitly demonstrate that there is no thermal oxidation between silicon surface and wet-chemically grown oxides because the passivation effect is mainly determined by the wet oxidation methods. Overall, a rather high temperature annealing process (700°C–900°C) is of paramount importance for the passivation quality of LPD SiO_2 film. And the enhanced passivation effect comes from the improved quality of the LPD SiO_2 film rather than the formation of thermal oxide.

3.3 Influence of H_2SiF_6 concentration

To study the effect of the H_2SiF_6 concentration on the properties of the LPD SiO_2 film, the other growth parameters, e.g., deposition temperature of 50°C, deposition time of 2 h were kept constant. As shown in Fig. 3(a), the thickness of the SiO_2 film first increases with the H_2SiF_6 concentration up to 1.5 M, suggesting an increased deposition rate in the concentration range. The reason for this is that the reversible reaction is promoted to the right side with increased H_2SiF_6 concentration, thus facilitating the precipitation of SiO_2, as expressed in Eq. (1). Then the thickness of the SiO_2 film remains around 150 nm in the range of H_2SiF_6 concentrations from 1.5 M to 2.0 M, achieving the maximum deposition rate of 75 nm/h.

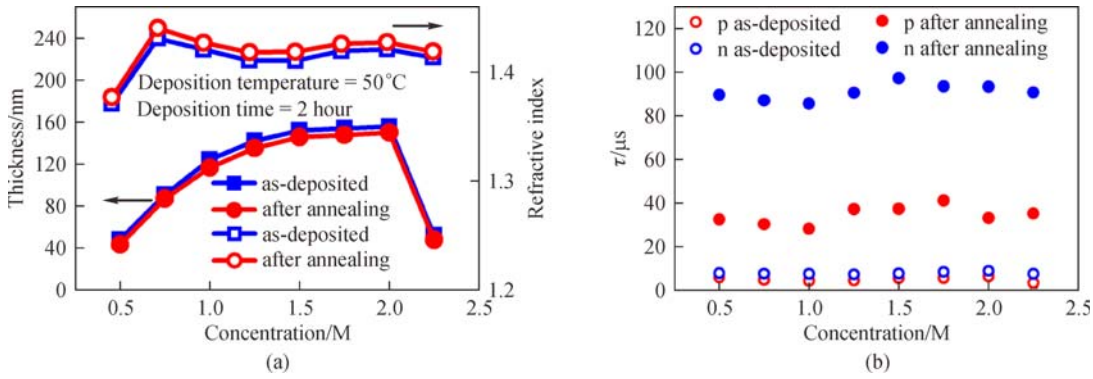

Fig. 3 Influence of H_2SiF_6 concentration on LPD SiO_2 film

(a) Dependence of the thickness and the refractive index of the as-deposited LPD SiO_2 film and the post-annealed LPD SiO_2 film on H_2SiF_6 concentration; (b) influence of H_2SiF_6 concentration on τ of the as-deposited and the post-annealed n-type and p-type samples

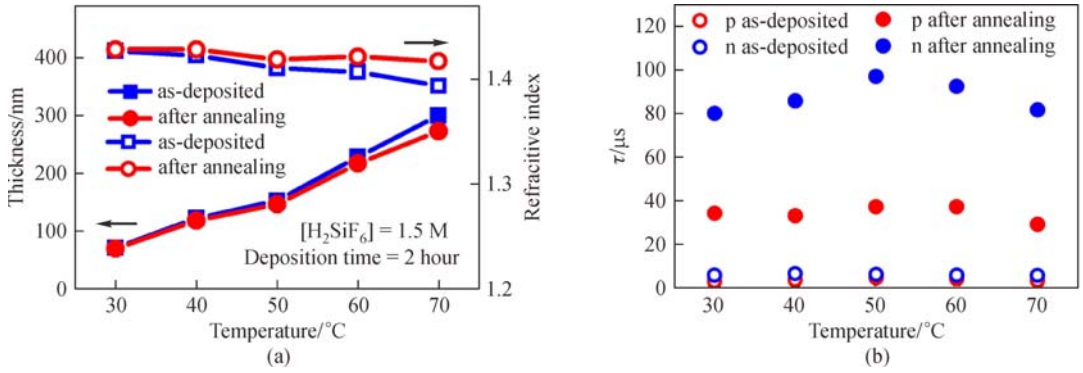

Fig. 4 Influence of growth temperature on LPD SiO_2 film

(a) Dependence of the thickness and refractive index of the as-deposited and post-annealed LPD SiO_2 films on the growth temperature; (b) Influence of growth temperature on τ of the as-deposited and post-annealed n-type and p-type samples

However, as further increasing the H_2SiF_6 concentration to 2.25 M, the film thickness decreases dramatically, which is ascribed to the insufficient H_2O (as a reactant) at an excessively high H_2SiF_6 concentration. From the result above, it can be inferred that the concentration of H_2SiF_6 has a great influence on the deposition rate of the LPD SiO_2 film and a concentration of 1.5 M may be a good choice as the growth condition considering both the process time and material cost. Regarding the refractive index, the value of the LPD SiO_2 film is between 1.41 and 1.43 (except the one grown with 0.5 M) as presented in Fig. 3(a), approaching to that of the thermally grown SiO_2 [21]. After annealing at 800°C, the refractive index of the LPD SiO_2 films is slightly increased while the thickness is decreased. The changes of the film thickness and the refractive index suggest the reconstruction of the LPD SiO_2 film, which may be largely caused by the decreased chemical bond of -OH and -F, incorporate in the as-deposited LPD SiO_2 films.

Figure 3(b) shows the τ of the samples with annealing and without annealing as a function of the H_2SiF_6 concentration. No matter it is n-type textured Si wafers or p-type polished Si wafers, the surface passivation quality of the as-deposited SiO_2 film is rather poor but dramatically enhanced after annealing at 800°C for 5 min in atmosphere, and does not exhibit much dependence on the concentration of H_2SiF_6. The excellent passivation effect on both n-type and p-type wafers suggests the chemical passivation mechanism of the LPD SiO_2 film. According to Eq. (2) [22],

$$\frac{1}{\tau} = \frac{1}{\tau_b} + \frac{2S}{W}, \tag{2}$$

where τ_b is the bulk lifetime of silicon wafer and τ is the measured effective minority carrier lifetime, W is the thickness of the silicon wafer, the τ_bs of n-type and p-type wafers are respectively obtained by iodine-ethanol passivation method and assuming the τ_bs are the same for each group of wafers, the average effective surface recombination velocities (S) of the LPD SiO_2 passivated n-type and p-type silicon wafers are calculated to be 110 and 260 cm/s, respectively. Obviously, the LPD SiO_2 film has a better passivation effect on the n-type wafer, even though its surface is textured, demonstrating that field-effect passivation also plays an important role in the passivation mechanism of LPD SiO_2 film.

3.4 Influence of growth temperature and application in solar cells

Keeping the H_2SiF_6 concentration of 1.5 M and the deposition time of 2 h, the influence of growth temperature on the properties of the LPD SiO_2 films was further studied in detail. As shown in Fig. 4(a), the thickness of the LPD SiO_2 films almost increases linearly with increasing temperature from 30°C to 70°C. Because the hydrolysis of H_2SiF_6 is an endothermic reaction and the solubility of SiO_2 in H_2SiF_6 decreases with the increased temperature, a higher growth temperature accelerates the precipitation of SiO_2 [8]. On the contrary, the refractive index of the SiO_2 films decreases with increased growth temperature. After annealing at 800°C for 5 min in atmosphere, all the SiO_2 films grown at different temperatures become thinner and denser. In addition, the influence of growth temperature on the refractive index is weakened. Though the deposition rate increases with growth temperature, the thermal cost also increases. Considering the tradeoff between thermal cost and deposition rate, the growth temperature of 50°C may be the optimal choice. Figure 4(b) illustrates the dependence of the τ of the p-type and n-type samples with and without annealing on growth temperature. After annealing, the τ of the p-type Si wafer passivated by LPD SiO_2 film reaches around 35 μs (except the one with the deposition temperature of 70°C), and that of the n-type samples is between 80 μs and 97 μs, both suggesting a good passivation quality of the LPD SiO_2 films. Similar to the dependence on the concentration of H_2SiF_6, the influence of growth temperature on the surface passivation effect is also not prominent.

All of the above results indicate that the prepared LPD SiO_2 film is suitable to be applied to silicon solar cells as an excellent surface passivation layer. Although the LPD SiO_2 film with a thickness of above 100 nm can be deposited to make it simultaneously act as an antireflection and passivation layer, it is too thick to be punctured by the silver paste, thereby leading to a severe contact problem. Therefore, in this study, the thickness of the SiO_2 film of about 5 nm was controlled to use it only as a passivation layer and SiN_x layer was still required to be deposited as the antireflection layer. It is worth mentioning that the LPD SiO_2 film with such thickness has almost an equal passivation effect to that with the thickness of several tens of nanometers. Furthermore, the SiN_x layer also has a contribution to the passivation through field-effect passivation. As a result, as shown in Fig. 5, the conversion efficiency of the LPD SiO_2 passivated solar cells reaches as high as 19.5% with an open circuit voltage of 641 mV, a short circuit current of 9.07 A and a fill factor of 80.2%.

4 Conclusions

The high quality SiO_2 film was successfully grown by a novel LPD technique and applied to silicon solar cells as the surface passivation layer. Compared to the common deposition method of SiO_2 film, the LPD is superior with an ultra-low growth temperature (50°C), a relative high deposition rate (75 nm/h), simple equipment and convenient operation. The prepared LPD SiO_2 film exhibits perfect coverage on textured silicon surface with high

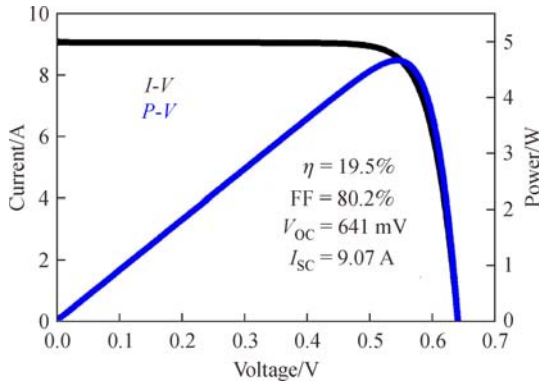

Fig. 5 *I-V* and *P-V* characteristics of the LPD SiO_2 passivated silicon solar cell on a large scale (156 mm × 156 mm)

elemental purity. The passivation quality of the LPD SiO_2 film is strongly improved with increased refractive index after annealing at a temperature higher than 700°C. It is important to find out that the LPD SiO_2 film can effectively passivate both the p-type and n-type Si wafers but results in a lower surface recombination velocity on n-type Si wafers, revealing the simultaneous existence of chemical passivation and field-effect passivation. In addition, although the deposition parameters have little influence on the passivation effect, they affect the deposition rate. An H_2SiF_6 concentration of 1.5 M and a deposition temperature of 50°C are proposed as the optimal deposition parameters based on the consideration of deposition rate and preparation cost. Finally, the LPD SiO_2 film were successfully applied to silicon solar cells as the front surface passivation layer and realized an efficiency of 19.5% on a large scale (156 mm × 156 mm). It is believed that the cost-effective passivation technique presented in this paper opens a new opportunity for high-efficiency silicon solar cells.

Acknowledgements This work was supported by the National Natural Science Foundation of China (Grant Nos. 61234005 and 11474201), and Shanghai Municipal Project (No.14DZ1201000).

References

1. Zhao J H, Wang A H, Green M A, Ferrazza F. 19.8% efficient "honeycomb" textured multicrystalline and 24.4% monocrystalline silicon solar cells. Applied Physics Letters, 1998, 73(14): 1991–1993
2. Schultz O, Glunz S W, Willeke G P. Multicrystalline silicon solar cells exceeding 20% efficiency. Progress in Photovoltaics: Research and Applications, 2004, 12(7): 553–558
3. Schultz O, Mette A, Hermle M, Glunz S W. Thermal oxidation for crystalline silicon solar cells exceeding 19% efficiency applying industrially feasible process technology. Progress in Photovoltaics: Research and Applications, 2008, 16(4): 317–324
4. Hoex B, Peeters F J J, Creatore M, Blauw M A, Kessels W M M, van de Sanden M C M. High-rate plasma-deposited SiO_2 films for surface passivation of crystalline silicon. Journal of Vacuum Science & Technology. A, Vacuum, Surfaces, and Films, 2006, 24(5): 1823–1830
5. Nagayama H, Honda H, Kawahara H. A new process for silica coating. Journal of the Electrochemical Society, 1988, 135(8): 2013–2016
6. Huang C J, Houng M P, Wang Y H, Wang N F, Chen J-R. Improved formation of silicon dioxide films in liquid phase deposition. Journal of Vacuum Science & Technology A, 1998, 16(4): 2646–2652
7. Huang C J. Quality optimization of liquid phase deposition SiO_2 films on silicon. Japanese Journal of Applied Physics, 2002, 41(Part 1, No. 7A 7A): 4622–4625
8. Yu S J, Lee J S, Nozaki S, Cho J. Microstructure developments of F-doped SiO_2 thin films prepared by liquid phase deposition. Thin Solid Films, 2012, 520(6): 1718–1723
9. Lin T, Jiang K, Zhou B X, Xu S F, Cai W B. Liquid-phase-deposited silicon oxide film as a mask for single-sided texturing of monocrystalline Si wafers. ACS Applied Materials & Interfaces, 2014, 6(2): 1207–1212
10. Huang C J, Chen J R, Huang S P. Silicon dioxide passivation of gallium arsenide by liquid phase deposition. Materials Chemistry and Physics, 2001, 70(1): 78–83
11. Wu H R, Lee K W, Nian T B, Chou D W, Huang Wu J J, Wang Y H, Houng M P, Sze P W, Su Y K, Chang S J, Ho C H, Chiang C I, Chern Y T, Juang F S, Wen T C, Lee W I, Chyi J I. Liquid phase deposited SiO_2 on GaN. Materials Chemistry and Physics, 2003, 80 (1): 329–333
12. Lee K W, Huang J S, Lu Y L, Lee F M, Lin H C, Huang J J, Wang Y H. Liquid-phase-deposited SiO_2 on AlGaAs and its application. Semiconductor Science and Technology, 2011, 26(5): 055006
13. Yuan H C, Oh J H, Zhang Y C, Kuznetsov O A, Flood D J, Branz H M. Antireflection and SiO_2 surface passivation by liquid-phase chemistry for efficient black silicon solar cells. In: 38th IEEE Photovoltaic Specialists Conference. Austin, TX, 2012, 686–689
14. He J, Ke Y C, Zhang G L, Deng Q C, Shen H, Lu S C, Qin M R, Wang X, Zeng C L. Liquid phase deposited SiO_2 on multi-crystalline silicon. Polymers Research Journal, 2015, 9: 57–65
15. Mansour A N. Characterization of NiO by XPS. Surface Science Spectra, 1994, 3(3): 231–238
16. Wang H L, Fang M S, Shi T J, Zhai L F, Tang C. Preparation of porous poly (lactic acid)/SiO_2 hybrid microspheres. Journal of Applied Polymer Science, 2006, 102(1): 679–683
17. Yeh C F, Chen C L, Lur W, Yen P W. Bond-structure changes of liquid phase deposited oxide ($SiO_{2-x}F_x$) on N_2 annealing. Applied Physics Letters, 1995, 66(8): 938–940
18. Grunthaner P J, Hecht M H, Grunthaner F J, Johnson N M. The localization and crystallographic dependence of Si subdioxide species at the SiO_2/Si interface. Journal of Applied Physics, 1987, 61(2): 629–638
19. Hiller D, Zierold R, Bachmann J, Alexe M, Yang Y, Gerlach J W, Stesmans A, Jivanescu M, Müller U, Vogt J, Hilmer H, Löper P, Künle M, Munnik F, Nielsch K, Zacharias M. Low temperature silicon dioxide by thermal atomic layer deposition: investigation of material properties. Journal of Applied Physics, 2010, 107(6): 064314
20. Lucovsky G, Mantini M J, Srivastava J K, Irene E A. Low-

temperature growth of silicon dioxide films: a study of chemical bonding by ellipsometry and infrared spectroscopy. Journal of Vacuum Science & Technology B, 1987, 5(2): 530–537

21. Pliskin W A, Esch R P. Refractive index of SiO_2 films grown on silicon. Journal of Applied Physics, 1965, 36(6): 2011–2013
22. Sproul A B. Dimensionless solution of the equation describing the effect of surface recombination on carrier decay in semiconductors. Journal of Applied Physics, 1994, 76(5): 2851–2854